Experimental Validation and Field Performance Metrics of a Hybrid Mobile Robot Mechanism

Pinhas Ben-Tzvi
Robotics and Mechatronics Laboratory, Department of Mechanical and Aerospace Engineering, The George Washington University, 801 22nd Street, NW, Washington, D.C. 20052
e-mail: bentzvi@gwu.edu

Received 17 October 2009; accepted 8 February 2010

This paper presents the experimental validation and field testing of a novel hybrid mobile robot (HMR) system using a complete physical prototype. The mobile robot system consists of a hybrid mechanism whereby the locomotion platform and manipulator arm are designed as one entity to support both locomotion and manipulation symbiotically and interchangeably. The mechanical design is briefly described along with the related control hardware architecture based on an embedded onboard wireless communication network between the robot's subsystems, including distributed onboard power using Li-ion batteries. The paper focuses on demonstrating through extensive experimental results the qualitative and quantitative field performance improvements of the mechanical design and how it significantly enhances mobile robot functionality in terms of the new operative locomotion and manipulation capabilities that it provides. In terms of traversing challenging obstacles, the robot was able to surmount cylindrical obstacles up to 0.6-m diameter; cross ditches with at least 0.635-m width; climb and descend step obstacles up to 0.7-m height; and climb and descend stairs of different materials (wood, metal, concrete, plastic plaster, etc.), different stair riser and run sizes, and inclinations up to 60 deg. The robot also demonstrated the ability to manipulate objects up to 61 kg before and after flipping over, including pushing capacity of up to 61 kg when lifting objects from underneath. The above-mentioned functions are critical in various challenging applications, such as search and rescue missions, military and police operations, and hazardous site inspections.

1. INTRODUCTION

Two decades ago, most mobile robots were slow-moving research platforms rolling through university corridors. Nowadays, mobile robots are starting to explore various outdoor environments for a variety of application domains, such as military, police, hazardous site exploration, surveillance, and reconnaissance. Some are intended to explore not only natural terrains, but also artificial environments, including stairs, ramps, cylindrical obstacles, large step obstacles, and ditches. Traversing such urban obstacles has been a great challenge and inevitable difficulty to the improvement of mobility and expansion of surveillance ranges for mobile robots.

The transition from "structured" to "unstructured" environments and, even more so, the requirement in some situations to "traverse" the obstacle rather than "avoid" it is one of the greatest challenges in the field because the physical interaction of the robot with the environment is in general very complex and strongly influences the overall system's performance. Thus, the introduction of robots to unstructured terrain has required fundamentally different approaches to mobility and manipulation in response to interaction with the environment.

Various designs of tracked mobile robots for unstructured environments have an optional feature in the design to attach a manipulator arm on top of the mobile platform as an add-on system or part of the platform. Some of these robots are PackBot (Yamauchi, 2004), Talon (Foster-Miller, 2010), AZIMUT (Michaud, Létourneau, Paré, Legault, Cadrin, et al., 2003), Andros Mark V (White, Sunagawa, & Nakajima, 1989), Matilda (Munkeby, Jones, Bugg, & Smith, 2002), Wheelbarrow MK8 (Costo & Molfino, 2004), LMA (Goldenberg & Lin, 2005), variable configuration VCTV (Iwamoto & Yamamoto, 1990), Helios VI and VII (Guarnieri, Debenest, Inoh, Fukushima, & Hirose, 2005; Hirose, Fukushima, Damoto, & Nakamoto, 2001), and Ratler (Purvis & Klarer, 1992). The designs of these mobile robots are mainly based on wheel mechanisms, track mechanisms, and a combination of both. Our focus is on tracked mobile robots that are capable of not only providing locomotion but also manipulation capabilities.

Increasingly, mobile robotic platforms are being proposed and used in rough terrain and high-risk missions for law enforcement and military applications [e.g., in Iraq for IED (improvised explosive device) detection], hazardous site cleanups, and planetary explorations (e.g., Mars Rover). These missions require the mobile robots to

perform difficult locomotion and dexterous manipulation tasks.

A mobile robot's structure typically consists of a mobile platform that is propelled with the aid of a pair of tracks, wheels (Angeles, 2005; Wang & Low, 2008), or legs (Kennedy, Agazarian, Cheng, Garrett, Huntsberger, et al., 2001; Saranli, Buehler, & Koditschek, 2001) and a manipulator arm attached on top of the mobile platform to provide the required manipulation capability (of hazardous materials, neutralization of bombs, etc). Several designs of mobile robots have pushed further the state of the art, such as PackBot (Yamauchi, 2004) and RHex (Saranli et al., 2001), to include the ability to return the robot platform when flipped over. However, this may not be possible if the robot is equipped with a manipulator arm. This issue is also addressed by the new design that provides locomotion and manipulation simultaneously and interchangeably.

A new technology of a hybrid mobile robot (HMR) design is presented. The new mobile robot design is based on hybridization of the mobile platform and manipulator arm as one entity for robot locomotion as well as manipulation. The paradigm is that the platform and manipulator are interchangeable in their roles in the sense that both can support locomotion *and* manipulation in several configuration modes. This paper focuses on presenting a series of extensive tests that were performed in order to qualitatively and quantitatively assess the robot's mobility and manipulation characteristics using a complete physical prototype. The obstacle course consisted of various test rigs including man-made and natural obstructions as a representative subset of possible hindrances to cross-country movement. Some of the obstacles and types of tests that were used in order to test and experimentally validate the HMR mechanism included the following:

(a) Ditch crossing: different ditch widths were tested.
(b) Step obstacle climbing and descending: different step obstacle heights were tested.
(c) Manipulation before and after flipping over.
(d) Traversing cylindrical obstacles of different diameters.
(e) Climbing and descending stairs of different materials (wood, metal, concrete, plastic plaster, etc.), stair riser and run sizes, and inclinations.
(f) Traversing rubble piles using locomotion and manipulation modes simultaneously.
(g) Lifting and carrying loads including testing pushing capacity from underneath objects.
(h) Speed runs.

Based on the extensive experimental testing, it was found that such a robot can adapt extremely well to various ground conditions to achieve performance necessary for challenging field operations such as search and rescue missions, reconnaissance, military and police operations, hazardous site inspections, and planetary explorations.

2. MOBILE ROBOT DESIGN

The mechanical design architecture of the HMR mechanism is briefly presented in this section in order to provide the reader with the necessary design details in terms of the overall mechanical design structure, such as the degrees of freedom (DOFs) the robot includes, joint torque capacities, physical dimensions, and overall weight. This section also presents the related control hardware architecture that supports the mechanical design and the various mobility and manipulation configuration modes the robot can exhibit. Further details of the mechanical design are available in Ben-Tzvi (2008) and Ben-Tzvi, Goldenberg, and Zu (2008a, 2008b).

The proposed design approach is twofold and is summarized as follows: (i) the manipulation and the locomotion platforms are integrated as one entity resulting in a hybrid mechanism rather than two separate and attached mechanisms. Consequently, the same joints that provide the manipulator's DOFs also provide the mobile platform's DOFs for locomotion. (ii) The overall mobile robot platform is designed in a *geometrically* symmetric manner in order to allow flip over and invertability with no need for added active means.

2.1. Mechanical Design Description

The overall mechanical design is depicted in Figure 1. If the platform is inverted due to flip over, the fully *geometrically symmetric* design [Figure 1(a)] allows the platform to continue to the destination with its new configuration with no need of returning. It is also able to deploy/stow the manipulator arm from both sides of the platform.

The mobile robot system is composed of two identical and parallel base link 1 tracks (left and right), link 2, link 3, end effector, and passive wheels. To support the symmetric nature of the design, all the links are nested into one another. Link 2 is connected between the two base link tracks via joint 1 [Figure 1(b)]. Passive wheels are inserted between links 2 and 3 and connected via joint 2, and another passive wheel is inserted between link 3 and the end effector via joint 3 [Figure 1(b)]. The passive wheels are used to support links 2 and 3 when used for various configuration modes of locomotion/traction. Link 2, link 3, and the end effector are connected through revolute joints, are able to provide continuous 360-deg rotation, and can be deployed separately or together from either side of the platform. To prevent immobilization of the platform during a flip-over scenario, rounded and pliable covers are attached to the sides of the platform as shown in Figure 1(a).

Excluding the end effector, the design includes four motors (including gear heads); two are situated at the back of each base link track to propel the racks independently and the other two at the front to propel joints 1 and 2 (Figure 2). All four motors at the base link tracks are identical brushless dc motors with a rated power of 363 W and

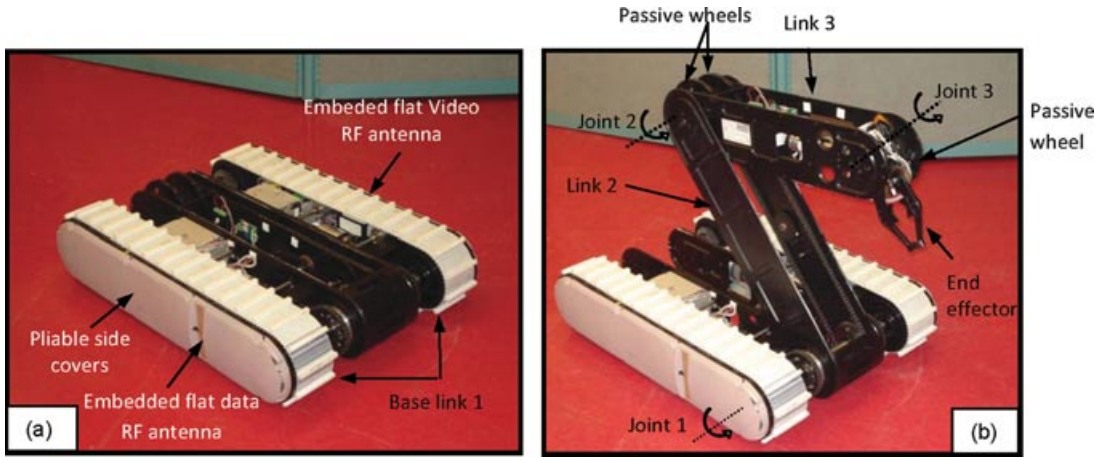

Figure 1. Mobile robot prototype: (a) stowed-links configuration mode; (b) open configuration mode (all other covers removed).

a continuous stall torque of 0.7 Nm. The motion from each motor at the back is transmitted through a 1:32 ratio planetary servo gear head and a 1:2 ratio bevel gear in order to transfer the motion in a 90-deg angle as well as to amplify the torque capacity required for propelling the pulleys that drive the tracks (Figure 2, Detail A). The motor at the front of each base link provides propulsion to one additional link (Figure 2, Detail B). The motion is transmitted through a 1:120 ratio harmonic drive and two additional transmission stages—namely, a 1:2 ratio bevel transmission followed by a 1:2.5 ratio chain and sprocket transmission in order to achieve greater torque capacities as required for each link 2 and 3. The required torque capacities were derived with the aid of the dynamic simulations (Ben-Tzvi et al., 2008a; Ben-Tzvi, Raoufi, Goldenberg, & Zu, 2007), which helped in selecting an appropriate combination of components such as motors and gear heads. Each of the motors is equipped with a spring-applied break in order to prevent unwanted

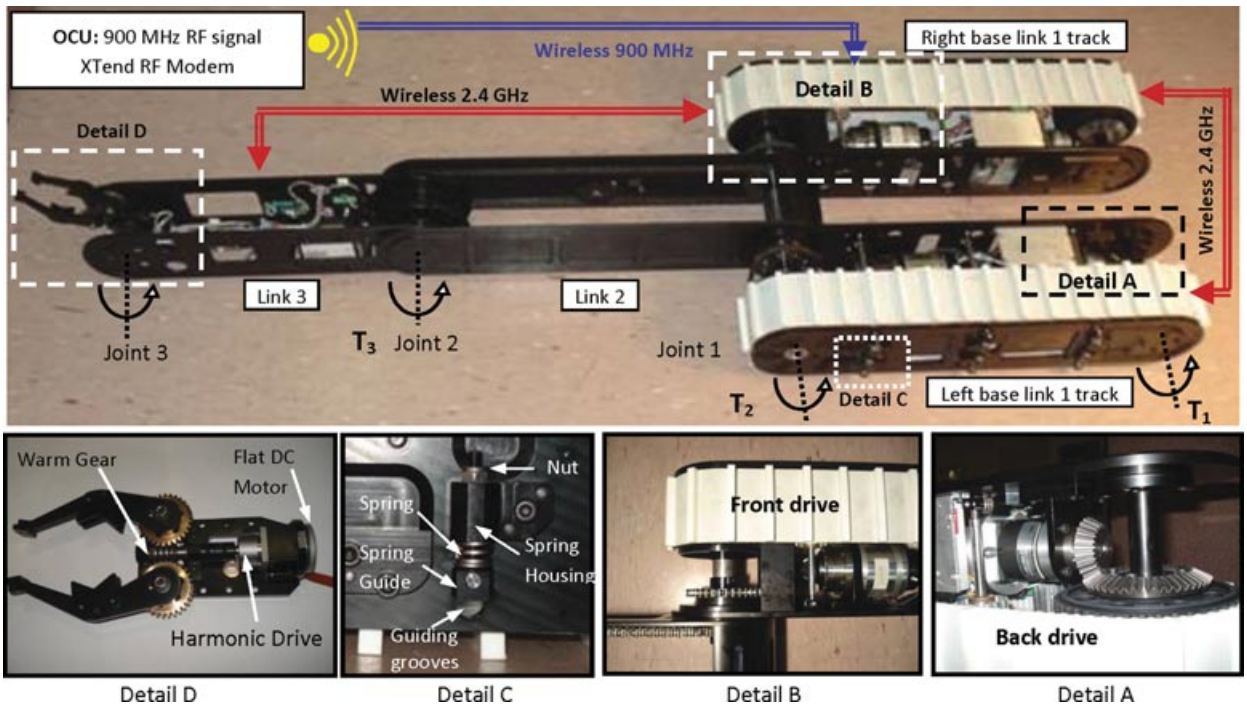

Figure 2. Onboard wireless communication layout and design details (all covers removed).

Table I. Robot design specifications

Specification	Value
Total mass (including batteries and electronics)	65 kg
Wheelbase/length (arm stowed)	635/814 mm
Length (arm deployed)	2,034 mm
Width (with pliable side covers)	626 mm
Height (arm stowed)	179 mm
Max. torque in joint 1: T_1	32 Nm
Max. torque in joint 2: T_2	157 Nm
Max. torque in joint 3: T_3	157 Nm
Speed of platform FWD/BKWD motion	Up to 1 m/s
Platform rotation speed	36 deg/s
Link 1 rotation speed about joint 1	30 deg/s
Link 2 rotation speed about joint 1	52 deg/s
Link 3 rotation speed about joint 2	52 deg/s
Gripper wrist rotation speed about joint 3	15 deg/s
Gripper open/close speed	8 deg/s

relative motion between links when the motors are idle, as well as a miniature optical encoder for position and velocity control purposes.

The gripper mechanism and its associated electronics and independent power sources are situated in the space available in link 3. For the existing design, the gripper has two DOFs and hence two additional motors and gear systems. The gripper submechanism is also designed to provide continuous rotations about joint 3 (Figure 2, Detail D) and hence can be deployed from either side of link 3. Rotation about joint 3 is generated with a dc micromotor connected to a planetary gear head and a bevel gear. The open/close motion of the gripper is implemented with a flat brushless dc motor connected to a miniature harmonic drive and a worm gear (Figure 2, Detail D). The design also includes a built-in dual-operation track tension and suspension mechanism (Ben-Tzvi et al., 2008a) situated in each of the base link tracks (Figure 2, Detail C). The suspension mechanism is also used to absorb some of the energy resulting from falling or flipping, thus providing some compliance to impact forces. Several dimensions of the mobile robot are provided in Table I. The overall size, especially the wheelbase/overall length, was determined based on predictable obstacle sizes (e.g., stairs, tables, typical household rubble) and other design considerations as discussed in Ben-Tzvi (2008) and Ben-Tzvi et al. (2008a, 2008b).

2.2. Description of the Control Hardware Architecture

The wireless and modular control hardware architecture designed for the HMR is depicted in Figures 2 and 3. This scheme provides onboard wireless control interfaces between the robot subsystems. The electrical hardware is distributed in three of the robot's segments (two base link tracks and link 3; see Figure 3). The electrical hardware associated with the gripper mechanism is situated in link 3 (Figure 2) and is not connected to any of the base link tracks via wires. Based on the mechanical design architecture of the HMR and the required functionality, the requirements for the control architecture include (i) the ability to provide continuous rotation between robot links without physical wiring or cable loops (which limit the robot link range of motion); (ii) modular mechanical and control system architecture, which provides operational fault tolerance—namely, if one of the robot subsystems fails during operation, others will continue to operate with no disruption; (iii) direct radio-frequency (RF) communication between each robot segment and the operator control unit (OCU) should be avoided in order to eliminate stand-alone

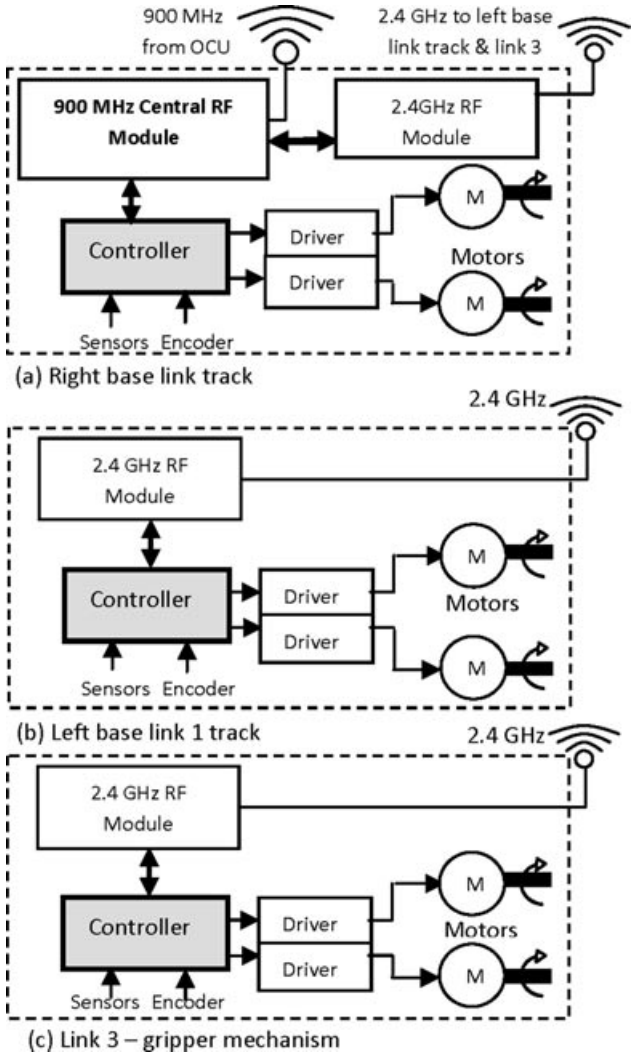

Figure 3. Hardware architecture for the HMR: (a) right base link track; (b) left base link track; (c) link 3, gripper mechanism.

vertically protruding antennas to maintain the overall structure's symmetry and prevent inconsistent data loss between the OCU and each link (may lead to desynchronization between the track and link motions). To address the above requirements, the following solutions have been implemented in the design: (i) include independent power source for each robot link; (ii) enable onboard wireless communication between robot links/subsystems to ensure that data pertaining to robot segments are received in one location and then distributed to others in a wireless manner.

2.2.1. Onboard Wireless RF Communication Layout

The right base link track contains a central RF module [Figure 3(a)] for communication with the OCU, and each of the remaining segments contains an RF module for onboard wireless RF communication. This, along with an independent power source in each segment, eliminates the need for physical wiring and slip ring connections between the rotating segments. This enables links 1, 2, and 3 and the gripper mechanism to provide continuous rotation about their respective joints and prevent any restriction to their range of motion.

Protruding antennas are avoided by designing flat antennas and embedding them into the robot side covers for wireless video communication and wireless data communication as shown in Figure 1(a).

As shown in Figure 2, the OCU includes a 900-MHz RF modem. The data transmitted by the stand-alone RF modem on the OCU are received by an RF module that is situated in the right base link track as shown in Figure 3(a). This RF module communicates with the local controller that controls the electronics (motors and associated drivers, sensors, etc.) in the right base link track and at the same time sends data pertaining to the other segments (left base link track and link 3) to a 2.4-GHz RF module in a wire connection. These data are then transmitted wirelessly to two other 2.4-GHz RF modules—one for the left base link track and the other for link 3 [Figures 3(b) and 3(c)], thus providing onboard wireless RF data communication among the robot joints. Further details of the control hardware architecture design and implementation are available in Ben-Tzvi (2008) and Ben-Tzvi, Goldenberg, and Zu (2007a, 2007b).

The robot is equipped with the following sensors: a tilt sensor; thermometer, global positioning system (GPS), three-axis compass (inclinometer), and battery-voltage monitor and two embedded cameras located in the front and back of the left base link track, which provide visual information to the OCU operator on the robot's surroundings.

2.2.2. Battery Power System

Each tracked link of the hybrid robot carries four nine-cell Li-ion battery packs in a series connection. Each Li-ion battery cell nominally provides 3.7 V at 2.4 Ah. A number of cells and protection circuits were used to achieve a specified current discharge of up to 15 A. This was implemented by constructing the nine-cell assembly of Li-ion battery cells in 3S3P construction (three of three cells connected in parallel were connected in series) resulting in a 11.1-V pack at 7.2 Ah. A 5-A max protection circuit module (PCM) was embedded in each parallel branch, which provides a total 15-A maximum current discharge. Four nine-cell packs, in a 4S construction, constitute the battery pack for each traction link (45 V nominal), which provide power to local motors and other electrical hardware. One nine-cell pack (12 V) is used as an independent power source for the gripper mechanism. The size of the battery pack is $110 \times 110 \times 70$ mm, and the overall weight is 1.6 kg. The designed battery packs provided the robot extended continuous operation of up to $\sim$2.5 h.

General specifications of the robot are summarized in Table I.

3. CONFIGURATION MODES OF OPERATION

The robot links can be used in three modes: (a) locomotion mode—all links used for locomotion to provide added level of maneuverability and traction; (b) manipulation mode—all links used for manipulation to provide added level of manipulation; (c) hybrid mode—combination of modes (a) and (b); whereas some links are used for locomotion, the rest could be used for manipulation at the same time; thus the hybrid nature of the mechanical design.

3.1. Robot Configurations for Manipulation

Figure 4 depicts different modes of configuration of the platform for manipulation purposes. Whereas some links are used as a platform for locomotion, others are used simultaneously for manipulation. In all configuration modes for manipulation, while links 2 and 3 are used for manipulation, the pair of base links can provide motion equivalent to a turret joint of the manipulator arm.

3.2. Mobility/Maneuverability Characteristics Testing and Validation

Figure 5 shows a series of configurations that demonstrate a number of basic functions the robot can provide in order to perform advanced mobility tasks. In subsequent sections, it will be demonstrated how these basic sets of configurations were utilized during the different stages of performing climbing of various obstacles as well as performing a variety of manipulation tasks. In these configurations link 2 is effectively used to support the platform for enhanced mobility purposes as well as climbing purposes. Link 2 also helps to prevent the robot from being immobilized due to high centering and also enables the robot to climb taller objects [Figure 5(b)]. Link 2 is also used to support the entire platform while moving in a tripod

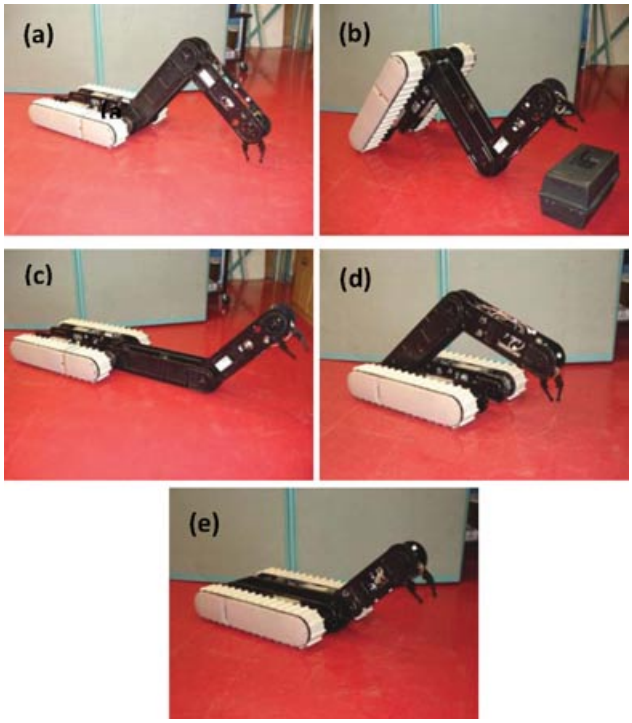

Figure 4. Robot configurations for manipulation.

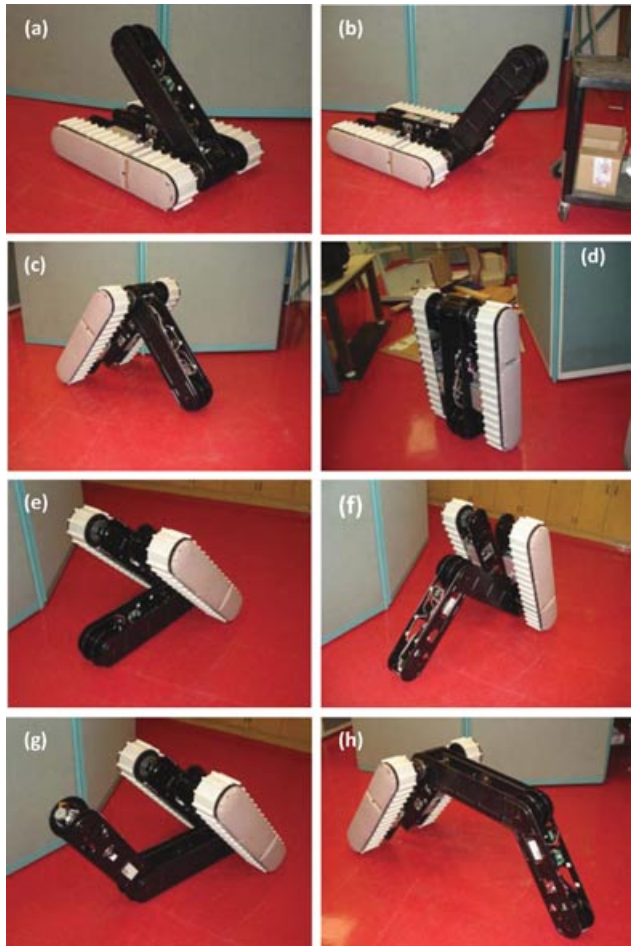

Figure 5. Configurations of the hybrid robot for mobility purposes.

configuration [Figure 5(c)]. The posture of the tripod configuration can be switched by rotating link 2 and passing it between the base link 1 tracks as shown in Figure 5(d) (without the robot falling). This functionality is effective when it is necessary to rapidly switch the robot's direction of motion in a tripod configuration. The configuration shown in Figure 5(e) demonstrates a very important and effective functionality whereby the entire platform (base link tracks) is lifted above the ground and rotated continuously about joint 1. This functionality is used to climb tall objects and cylindrical obstacles, as will be demonstrated in subsequent sections. Figure 5(g) shows how the passive wheels attached at the end of link 3 can be used to mobilize the entire platform while in motion.

3.3. Traction Configurations

Figure 6 shows several configurations for enhanced traction. For enhanced traction, link 2 and if necessary link 3 can be lowered to the ground level as shown in Figures 6(a) and 6(b). At the same time, as shown in configuration (c), the articulated structure of the mobile platform allows it to be adaptable to different terrain shapes and ground conditions. The passive wheels located at joints 2 and 3 provide additional support to the entire platform for generating different traction configuration modes. The hybrid nature of the robot can increase traction by using the manipulator's DOFs to pull the robot through debris. This feature is discussed in greater detail in Section 5.3 (as demonstrated later in Figure 22).

4. OCU AND ROBOT DOF COORDINATION

Two control sticks are included in the OCU (Figure 7) in order to coordinate the robot DOFs when generating the motions required for a given task. The forward, backward, right turn, and left turn motions of the base link tracks are controlled by an up, down, right, and left movement of the first control stick (C1), respectively. The second control stick (C2) is used to control link 2 and 3 DOFs. A right movement of the C2 control stick will generate a clockwise (CW) independent motion of link 2, and a left movement of the control stick will generate a counterclockwise (CCW) independent motion of link 2. Similarly, an up-and-down movement of the second control stick will generate an independent CW and CCW motion of link 3, respectively.

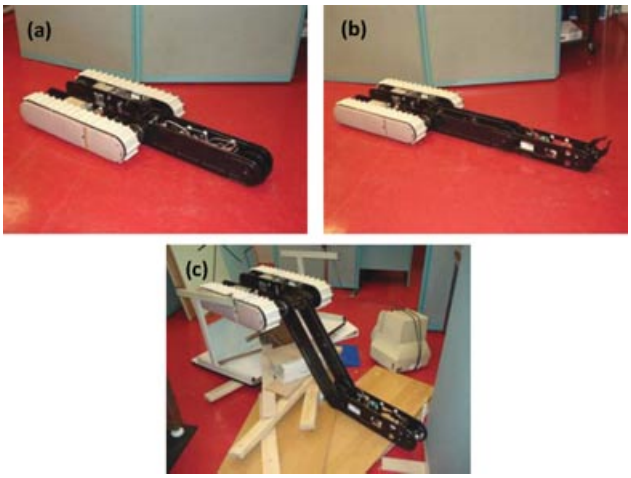

Figure 6. Configurations for enhanced traction.

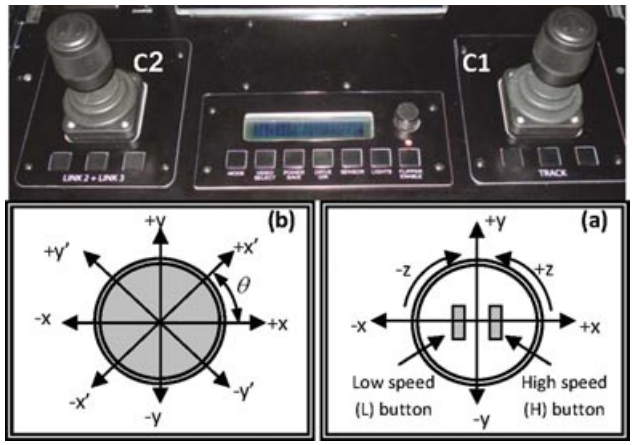

Figure 7. OCU and robot DOF: (a) control stick 1 (C1) motion layout; (b) control stick 2 (C2) motion layout.

Furthermore, four diagonal movements of the second control stick (i.e., $+x'$, $-x'$, $+y'$, $-y'$ directions as shown in Figure 7) will generate simultaneous motions of links 2 and 3 as summarized in Table II.

The CW and CCW wrist motions of the gripper mechanism as well as the open-and-close motions of the gripper jaws are generated with a separate mode of the first control stick.

The first and second control sticks can be operated simultaneously by the operator in order to provide simultaneous motions of the tracks along with different motion combinations of links 2 and 3, as explained above.

The above motion procedures are summarized in Figure 7 and Table II. Figure 7 shows the top view of control stick 1 (C1) with two switchable modes as follows: (i) track motions, mode 1 (M1); and (ii) gripper mechanism motions, mode 2 (M2). Control stick 2 (C2) has two coordinate systems x–y and x'–y' for link 2 and 3 motions. The control angle θ in C2 provides speed variability to each of the links 2 and 3 when operated simultaneously.

To effectively control the various robot joint functionalities, in some cases the operater would need to learn to operate control sticks C1 and C2 simultaneously. This requires some training for the operator to learn and practice the motions as shown in Figures 7(a) and 7(b). For ease of use during operation, this layout is also available on the OCU itself.

5. EXPERIMENTAL SETUP AND RESULTS

A series of extensive experimental tests were performed to assess the robot's mobility, manipulability, and durability characteristics. The obstacle course consisted of various test rigs including man-made and natural obstructions as a representative subset of the robot's possible hindrances to cross-country movement related to pertinent applications, such as search and rescue, reconnaissance, surveillance, hazardous site inspections, and military and police missions. The key features that significantly enhanced the mobile robot's functionality were the ability to generate continuous rotations to each of its links without limiting

Table II. Robot motion specifications

	FWD	BWD	Right	Left
Tracks motions	C1 + M1 ($+y$) H/L	C1 + M1 ($-y$) H/L	C1 + M1 ($+x$) H/L	C1 + M1 ($-x$) H/L
	Wrist CW	Wrist CCW	Gripper jaws open	Gripper jaws closed
Gripper	C1 + M2 ($+y$)	C1 + M2 ($-y$)	C1 + M2 ($+z$)	C1 + M2 ($-z$)
	CW	CCW	CW/CCW	CCW/CW
Link 2 alone	C2 ($+x$)	C2 ($-x$)	N/A	N/A
Link 3 alone	C2 ($+y$)	C2 ($+y$)	N/A	N/A
Links 2 + 3	C2 ($+x'$)	C2 ($-x'$)	C2 ($+y'$)	C2 ($-y'$)

their range of motion and the ability to deploy the base link tracks, link 2 and 3 independently from the front and the back with various link sequences. The other important key feature is the overall geometrically symmetric design [in stowed links configuration; Figure 1(a)] that allowed the platform to invert itself and continue to operate with no need for special-purpose active means to reinvert it.

5.1. Robot Mobility Testing

Different types of terrains, such as flat roads, obstacles, stairs, ditches, rubble piles, and ramps, were tested with different shapes and sizes. These types of obstacles are typical challenges that mobile robots face during applications for search and rescue, reconnaissance, military operations, hazardous site inspections, etc. By providing the new locomotion and manipulation capabilities with the HMR system, the functionality performance of mobile robots in those applications is expected to be dramatically improved.

Some of the challenging tests that were used on the hybrid robot are as follows (the experimental results are also summarized later in a graphical format in Figure 19):

(a) Traversing cylindrical obstacles of different diameters. The experiments prove that the hybrid robot is able to traverse cylindrical obstacles up to 0.6-m (24 in.) diameter.
(b) Climb and descend stairs of different materials (wood, metal, concrete, plastic plaster, etc.), different stair riser and run sizes, and inclinations up to 60 deg.
(c) Step obstacle climbing and descending: different heights of step obstacles were tested. According to the experimental results, the hybrid robot could climb and descend steps up to 0.7-m (28 in.) height.
(d) Ditch crossing: different widths of ditches were tested. According to the experimental results, the hybrid robot could cross at least a 0.635-m (25 in.)-wide ditch.
(e) Lift and carry loads including testing pushing capacity from underneath objects up to 61 kg (~135 lb).
(f) Ability to provide manipulation functionality before and after flipping over.
(g) Inclined ramp adjustable from 0 to 60 deg with and without payloads.

5.1.1. Traversing Cylindrical Obstacles

The segmented nature of the robot's structure allows it to be able to surmount cylindrical obstacles such as pipes and tree logs up to 0.6 m in diameter. Figure 8 depicts several configuration steps to accomplish such tasks as follows: the base link tracks are deployed until they touch the obstacle [(a)–(c)]; at that point, the tracks start to propel the platform while at the same time they continue their rotation about joint 1 [(d)–(f)]. Only the combination of these simultaneous motions provides the robot with the ability to surmount such obstacles.

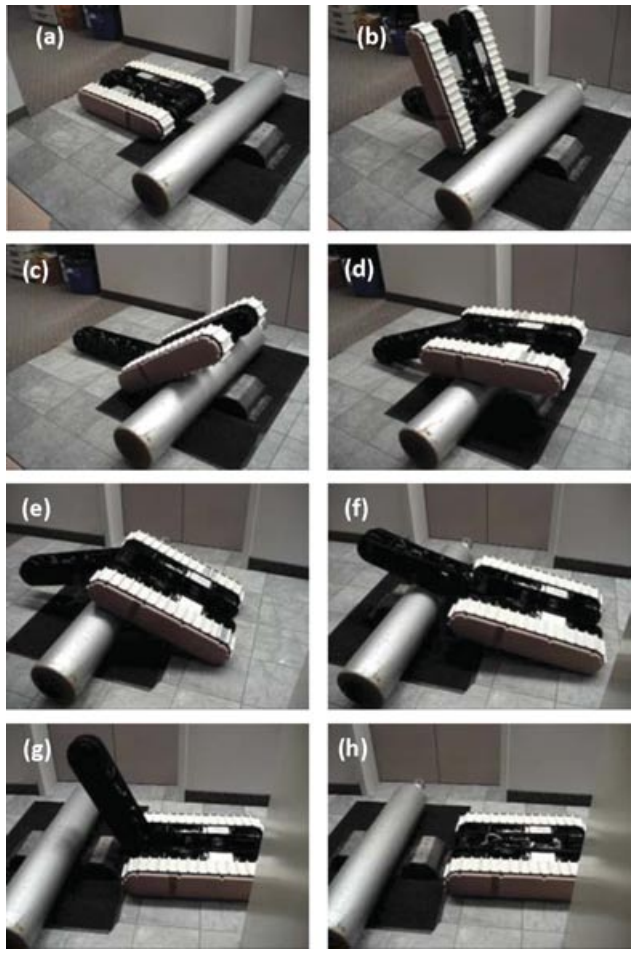

Figure 8. Surmounting cylindrical obstacles.

5.1.2. Stair Climbing

Figure 9 shows a series of motions the different links along with the tracks need to undergo in order to climb the stairs. The steps are as follows: the base link tracks are first deployed until they touch the stairs [(a)–(c)]; link 2 is closed, and the robot starts climbing with the tracks [(d)–(e)]; at the end of the stairs link 3 opens (f) to support the platform while the robot is in motion until position (g); link 3 rotates (until closed) to lower the robot until the tracks are in full contact with the ground (h).

5.1.3. Stair Descending

The steps the robot needs to undergo in order to descend stairs as shown in Figure 10 are as follows: link 2 is deployed until it touches the stairs [(a)–(b)]; the robot advances until the entire platform is on the stairs (c); link 2 closes (d); and the platform descends the stairs. Link 3 can

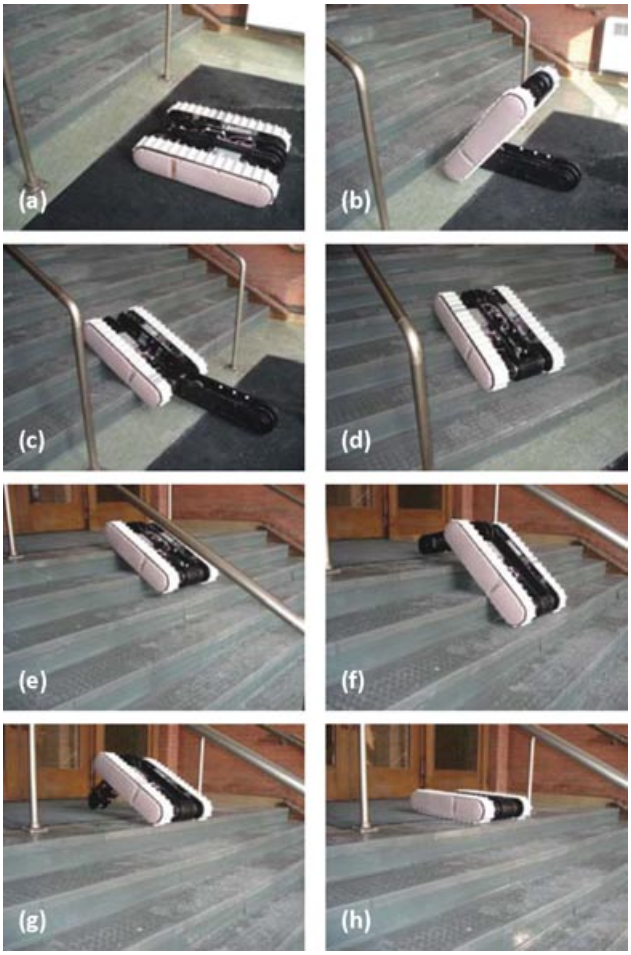

Figure 9. Stair climbing.

be deployed from the back in cases in which smooth landing from the stair edge is required [(e)–(f)].

5.1.4. Stair Descending: Other Configurations

Figure 11 depicts other configurations for stair descending. In both cases the descending stage is performed by deploying links 2 and 3 together in order to support the entire platform while descending. The difference between the steps shown in each case is the platform's initial orientation with respect to the stairs. These configurations are in particular useful in cases when the last step edge is much taller than the preceding steps. In this case the motion sequence of the robot links is as shown for the case when descending a step obstacle [steps (f)–(i) later in Figure 15].

5.1.5. Step Obstacle Climbing

Climbing step obstacles can be performed is several ways with the hybrid robot. These include (i) climbing with the base link tracks; (ii) climbing with link 2; and (iii) climbing with link 3. The climbing process with the first two options is described in detail in the following sections. The only difference between climbing with link 2 or 3 is the maximum step height because link 3 is shorter than link 2.

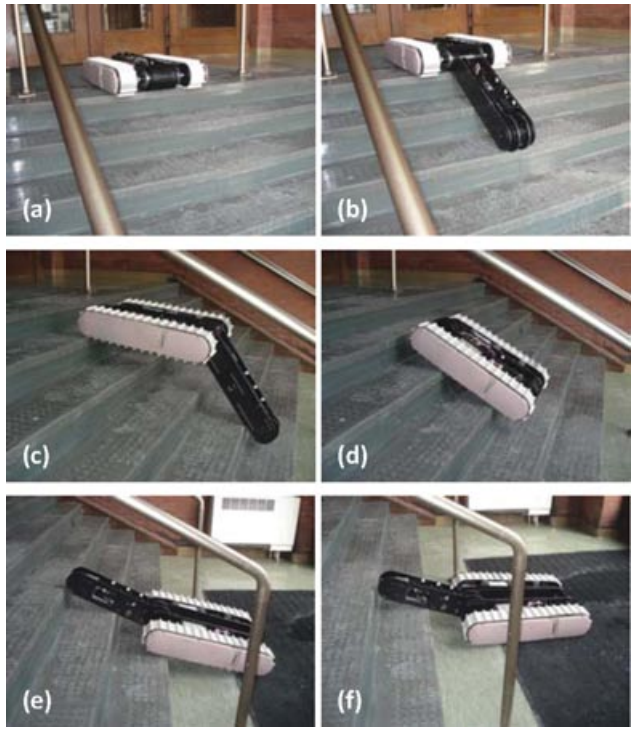

Figure 10. Stair descending.

Climbing with Tracks

Figure 12 shows series of motions in order to climb a 0.7-m step obstacle with the base link tracks. The steps are as follows: the base link tracks are first deployed on the step [(b)–(c)]; link 2 continues to rotate until the base link tracks adjust with the profile of the terrain (d); the platform advances to accomplish the climbing process (e), and link 2 closes (f). This climbing can also be accomplished with link 3 by interchanging the roles of links 2 and 3 (in this case, the back of the robot will be facing the step obstacle).

Climbing with Link 2

Similarly, Figure 13 shows a series of configurations the robot needs to undergo in order to climb the step obstacle with link 2 while link 3 is deployed from the back to support the entire platform to complete the climbing process. The configurations required in this case are (a)–(f), (j), and (k). This climbing can also be achieved with link 3 by interchanging the roles of links 2 and 3 (in this case, the back of the robot will be facing the step obstacle).

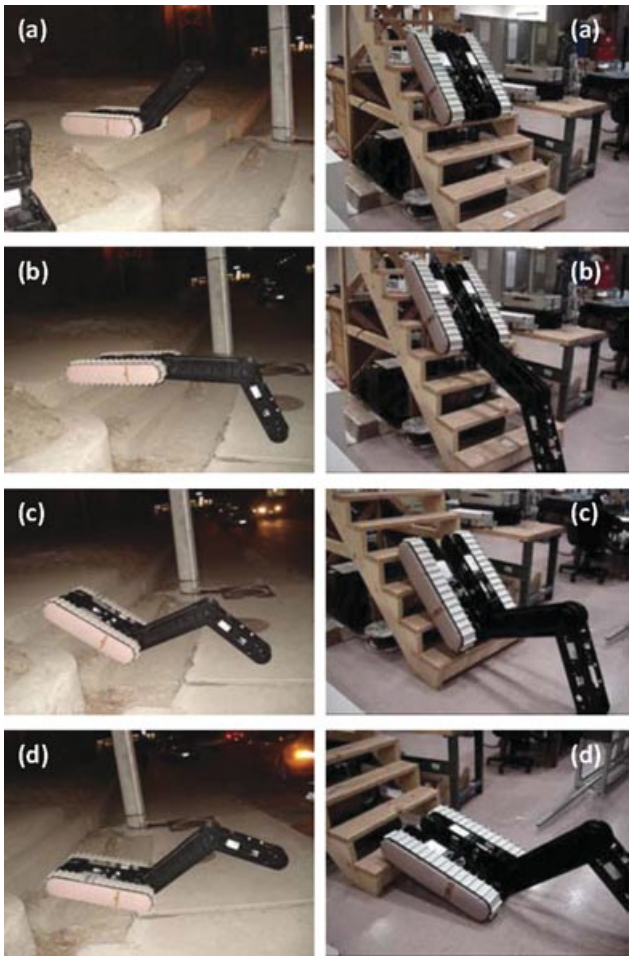

Figure 11. Stair descending: other configurations.

Figure 12. Step obstacle climbing with tracks.

The climbing process can also be accomplished with the tracks by including configuration (g)–(i) immediately after configuration (f) instead of skipping to configuration (j).

5.1.6. Step Obstacle Descending

Descending step obstacles can be performed in several ways with the hybrid robot. Some of the possible ways are (i) descending with links 2 and 3 and (ii) descending with the base links. These descending options are described in detail in the following sections.

Descending with Links 2 and 3

Figure 14 shows series of motions in order to descend a step obstacle with links 2 and 3. The steps are as follows: link 2 is deployed until it touches the ground to support the front of the robot when advancing forward [(b),(d)] [link 3 can also be deployed, as shown in configuration (c), in cases when the step to be descended is taller than the length of link 2]; link 2 rotates to lower the front of the platform (d); link 2 fully closes (e); link 3 opens to provide support while the robot moves forward [(f),(g)]; link 3 rotates (until closed) to lower the robot until the tracks are in full contact with the ground [(h)–(i)].

Descending with Base Link Tracks

Figures 15 and 16 show a series of motions in order to descend a step obstacle with the base links. The difference between the motion sequences in each case depends on whether the front end or the back end of the robot is facing the step to be descended. If climbing was performed with the base link tracks (Figure 12), then the back end of the robot will be facing the step edge. In this case the platform will need to reconfigure itself such that descending is performed with the robot front end in order to be able to deploy and use both links 2 and 3 in the descending process as shown in Figures 15 and 16. The reconfiguration can be done in two ways.

In the first way, the base link track will be rotated 180 deg about joint 1 until the tracks flip on the obstacle as shown in configurations (b)–(d) in Figure 15. The rest of the steps are as follows: links 2 and 3 are deployed until they touch the ground to support the robot when advancing [(e),(f)], link 2 rotates to lower the front of the platform (g), and the base link tracks continue to rotate until the tracks are in full contact with the ground [(h),(i)].

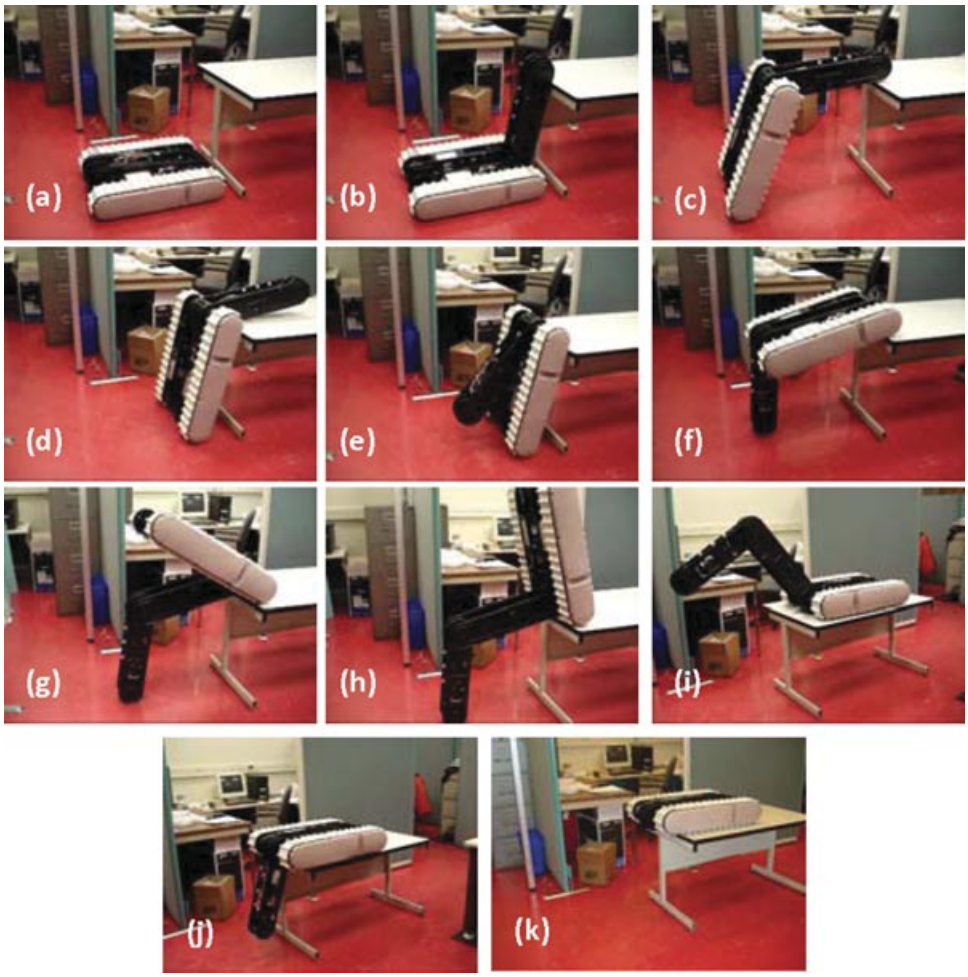

Figure 13. Step obstacle climbing with links 2 and 3.

In the second way, the entire platform will be rotated 180 deg on the obstacle such that the front end of the platform will be facing the edge of the step to be descended [Figure 16(a)]. The rest of the steps are similar to the ones shown in Figure 15.

5.1.7. Ditch Crossing

Ditches up to 0.635 m in width can be easily traversed because the robot can deploy link 2 from the front and link 3 from the back (when all links are stowed), as shown in Figure 17. The steps involved are as follows: from the back edge of the ditch, link 2 is deployed with or without link 3 (b); the robot advances until the front and back pulleys are supported by the ditch edges (c); link 2 closes and link 3 opens from the back (d); the robot continues its forward motion until the center of gravity (COG) passes the front edge of the ditch while link 3 prevents the robot from falling into the ditch when the COG is before the front edge [(e)–(f)]; and link 3 closes [(g)–(h)].

5.1.8. Platform Lifting and Carrying Capacity Testing

In cases in which it is required to remove objects or lift heavy objects from underneath, the compact and symmetric structure of the robot and the increased actuator strength due to the hybrid structure allow it to go under objects and lift as shown in Figure 18. According to the lifting experiments performed, the hybrid robot was able to lift objects weighing up to 61 kg (~135 lb). Various other experiments were also performed in order to test the platform's load capacity. On one occasion the robot was able to carry two people standing on the robot with the OCU on top, which accounted for an overall weight of 187 kg (411 lb).

The graphical representation of some of the above results is summarized in Figure 19 in order to show the

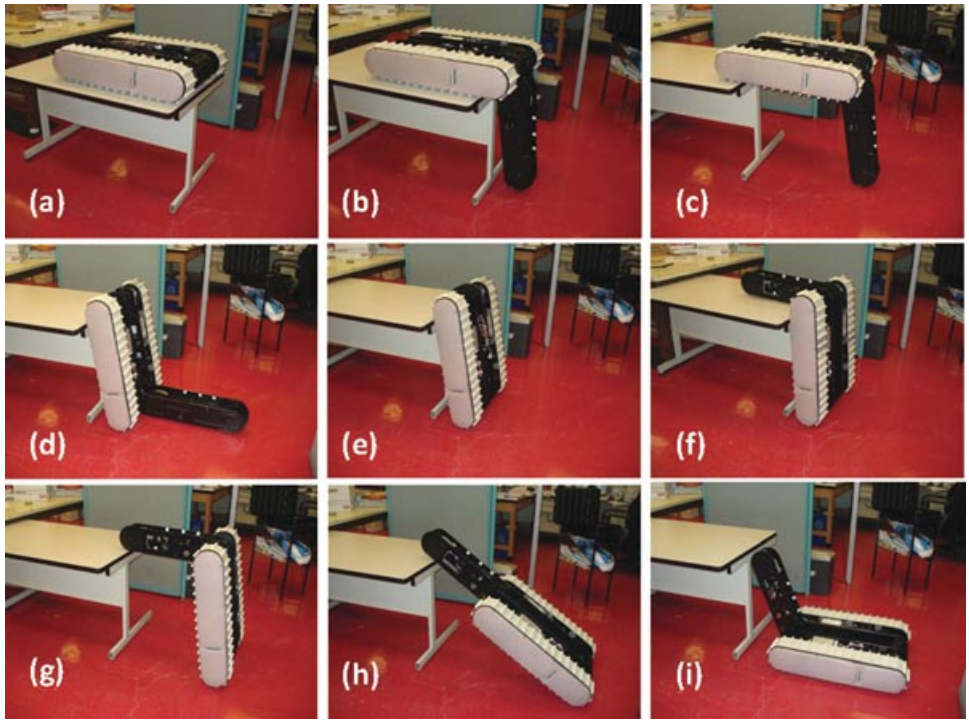

Figure 14. Step descending with links 2 and 3.

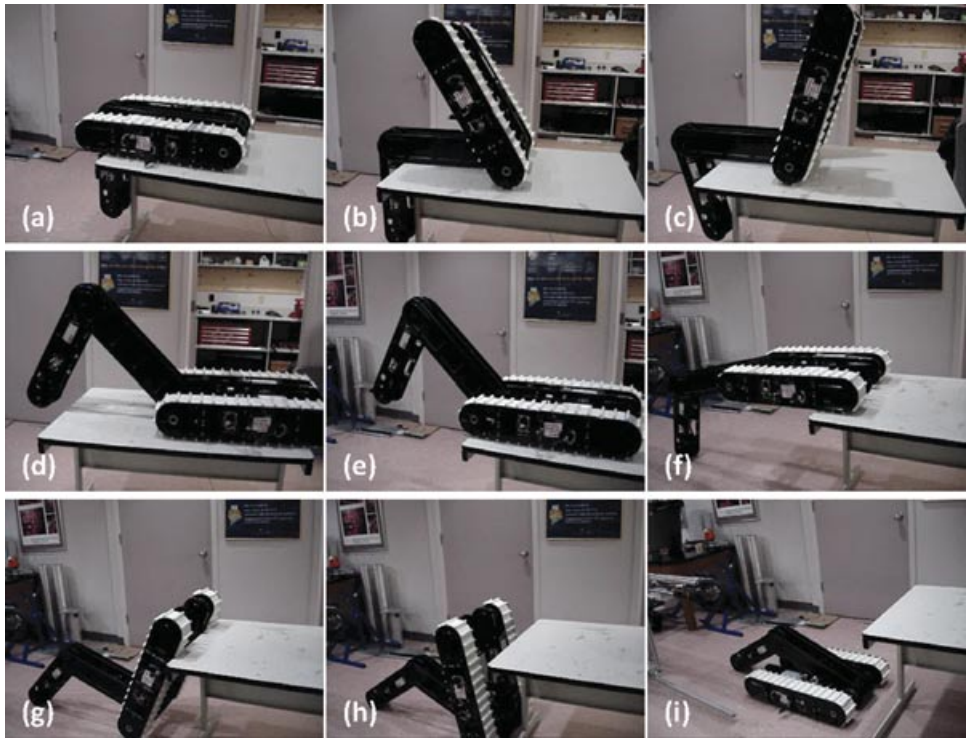

Figure 15. Step descending with base link tracks: tracks flip on the table.

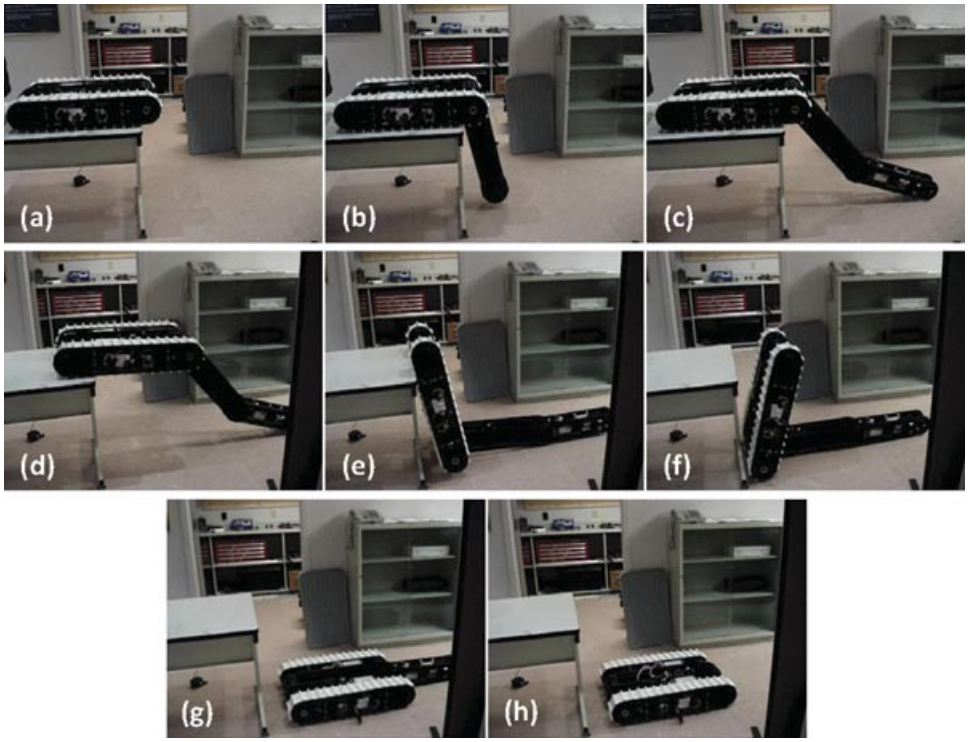

Figure 16. Step descending with base link tracks: tracks rotate on the table.

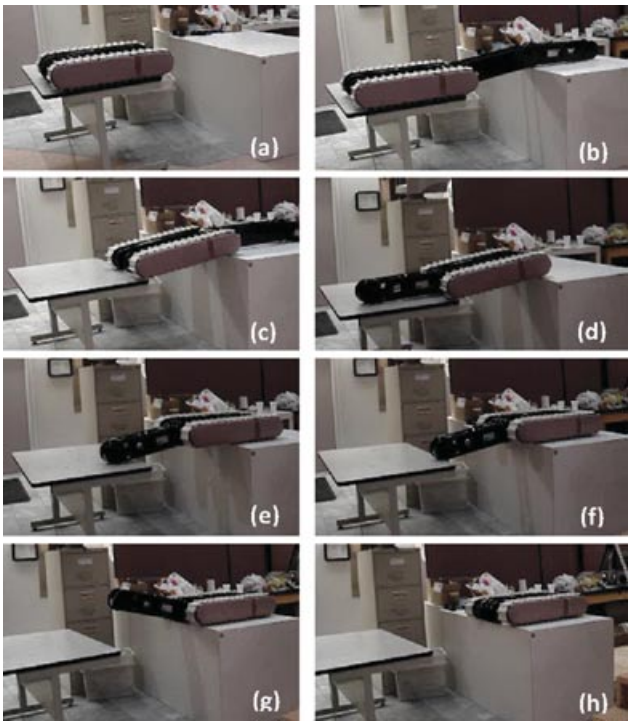

Figure 17. Ditch crossing.

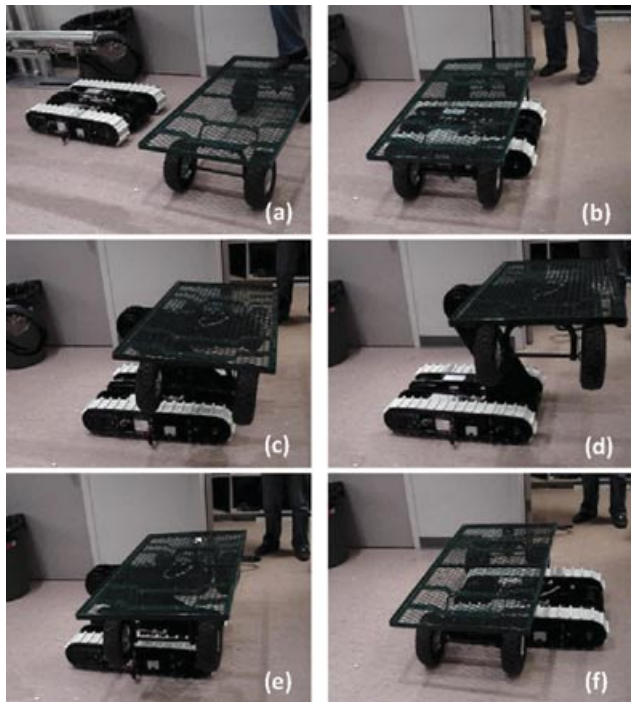

Figure 18. Lifting capacity testing.

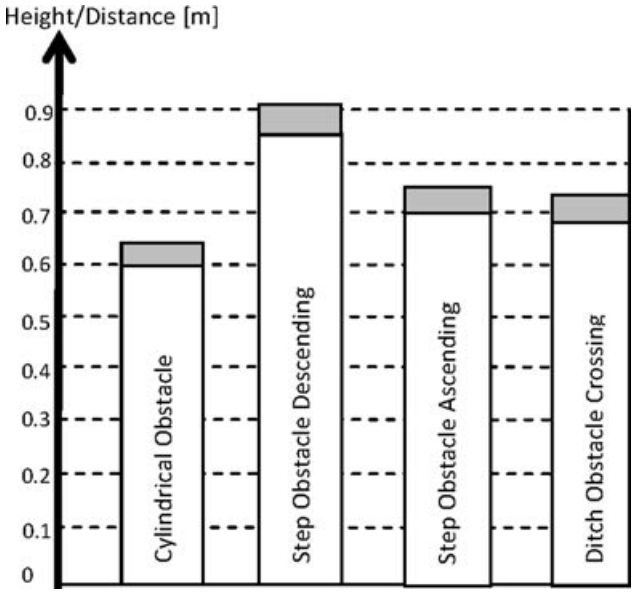

Figure 19. Experimental results: metrics for obstacle traversal.

height/distance variances between different tasks. The white regions represent the "safe region" where the robot was always able to successfully accomplish the prospective task without any failure for the same obstacle in each scenario. The "safe region" in each scenario described in Figure 19 represents at least 20 successful trials of the same obstacle. The gray region represents a feasible height/distance region as well, but the task's successful accomplishment was not guaranteed—namely, a 40%–50% failure rate was observed (i.e., for every 10 trials, the robot was not able to climb about four to five times). Beyond the gray region, the robot failed to accomplish the prospective task due to physical limitations of the link length and interactive conditions between the links and the obstacle (mainly due to insufficient traction).

To test the system's ability to overcome subsystem failure [as per requirement (2) in Section 2.2—operational fault tolerance capability], the communication to the motor that drives the left or right track was deliberately interrupted in some of the experiments (e.g., when the robot was descending the table as shown in Figure 15 or when the robot was crossing the ditch as shown in Figure 17). It was observed that the motion of the right or left base link track alone was sufficient to uninterruptedly change the configurations of the robot. The rest of the links functioned properly to successfully complete the required robot motions.

5.2. Concurrent Manipulation and Locomotion

Manipulation of objects can be incorporated simultaneously with the climbing and descending tasks presented in the preceding section. Several experiments were performed in order to demonstrate this capability, which is a direct outcome of the hybrid nature of the platform and manipulator arm and their ability to be interchangeable in their roles and to be able to provide both functionalities simultaneously.

Several locomotion tasks were successfully experimented while simultaneously manipulating an object. These include (i) ascending and descending of stairs; (ii) traversing tall cylindrical obstacles; (iii) crossing ditches; and (iv) climbing and descending step obstacles with various motion configurations.

To illustrate this capability, Sections 5.2.1 and 5.2.2 present two cases in which the robot climbed and descended a 0.7-m step obstacle while holding an object.

5.2.1. Concurrent Object Manipulation and Obstacle Climbing

Figure 20 shows the robot picking up an object and climbing a step obstacle with the base link tracks while holding the object with the gripper mechanism. This step climbing is similar to the one shown in Figure 12 with the exception that link 3 remains deployed in order to manipulate the object simultaneously.

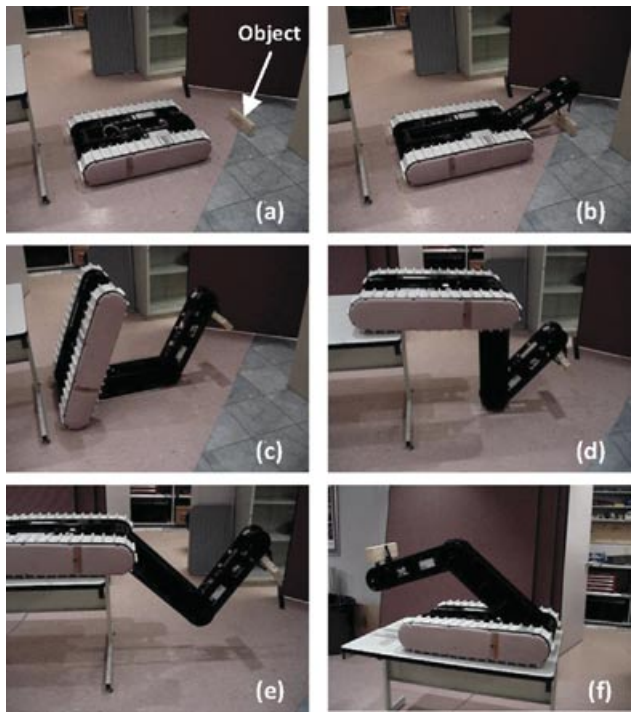

Figure 20. Concurrent climbing and manipulation.

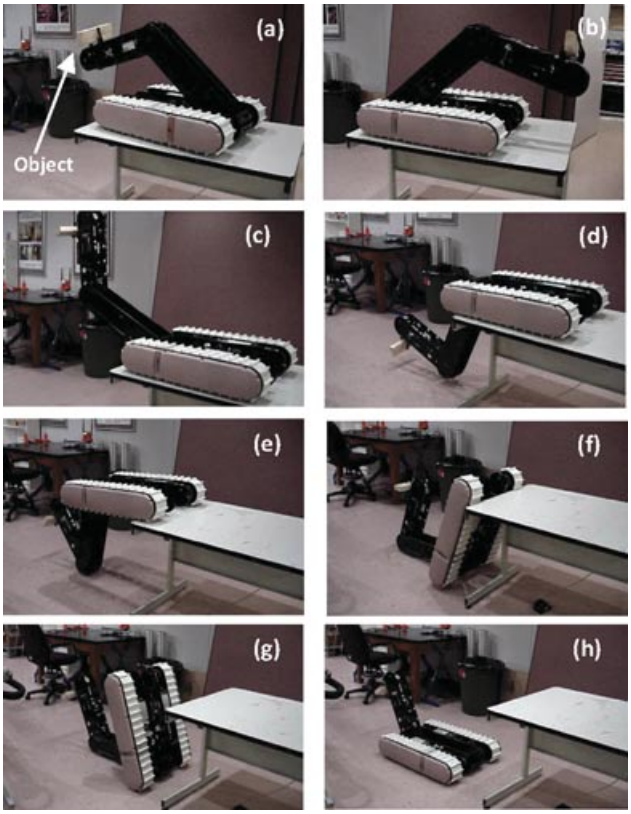

Figure 21. Concurrent descending and manipulation.

5.2.2. Concurrent Object Manipulation and Obstacle Descending

The HMR's configuration steps to descend the step obstacle with the base link tracks while holding the object with the gripper mechanism are shown in Figure 21. The motion sequence of the robot links required to descend the obstacle is similar to the one presented in Figure 15 with the exception that link 3 remains deployed in order to manipulate the object simultaneously.

5.3. Mobility Configurations for Rubble Pile Traversal

Figure 22 shows a simulated earthquake scenario in an office building with the robot's task being to traverse a rubble pile in its way to access and reach a target and search for survivors. This scenario demonstrates the hybrid robot's capability to easily climb over the rubble pile and return by using all the links interchangeably with a combination of the various mobility capabilities presented thus far. These mainly include climbing and descending with the aid the base link tracks, links 2 and 3. Some of the configuration steps in Figure 22 also show how the platform utilizes its ability to adjust the level of traction (due to the robot's articulated structure and the ability to change the relative absolute angle between two consecutive links) to effectively traverse the rubble pile.

5.4. Payload Capacity of End Effector for Manipulation

The experiments in this section demonstrate the considerably increased actuator strength capacity (in terms of joint torques) for manipulation purposes due to the articulated hybrid mechanical structure. The end-effector load capacity for different manipulation configurations was also evaluated. The graph shown in Figure 23 describes the load capacity of the end effector for several possible manipulation configurations.

Other configurations can be generated in the range of the configurations shown in the figure, such as vertical or horizontal reach. In some of the cases, the limiting factor in testing the end-effector payload capacity was the robot's ability to sustain structural stability (e.g., tilt forward due to the heavy payload at the end effector). In other cases, joint torque capacities of links 2 and 3 were the limiting factor to sustain a given payload at the end effector for a given configuration for manipulation purposes.

According to the graph in Figure 23, for a given torque capacity in joint 1, configuration (d) is optimal with a maximum dynamic payload capacity of ∼61 kg (∼135 lb) due to its noticeably greater resistance to tip-over instability. This payload capacity can be increased if joint 1 torque capacity is increased. The end-effector load capacity with configuration (a) is the least due to the robot's tendency to tip forward (tip-over instability) beyond a load of ∼14 kg (31 lb).

Depending on the required level of mobility, for greater payload requirements, either of configurations (b), (c), and (e) can be employed. In each of these configurations, a payload of ∼30 kg (66 lb) can be manipulated by the robot. These load capacities are limited by the joint capacity rather than the robot's tip-over stability, but they can be increased if joint 1 and 2 torque capacities are increased.

5.5. Adaptable Manipulation

As shown in the preceding section, the end-effector load capacity with configuration (a) shown in Figure 23 is the lowest due to the robot's tendency to tip forward beyond a load of 14 kg (∼31 lb). Tip-over instability becomes even more dominant for a given load when links 2 and 3 further extend forward without touching the ground [Figure 24(a)]. In these situations, the robot's articulated structure will readjust its configuration automatically. That is, when the system feels that it loses the balance, the platform relocates its COG to provide or compensate for the required counterforce moment.

One example of the adaptable manipulation capability is depicted in Figure 24, and the steps involved in this case are as follows:

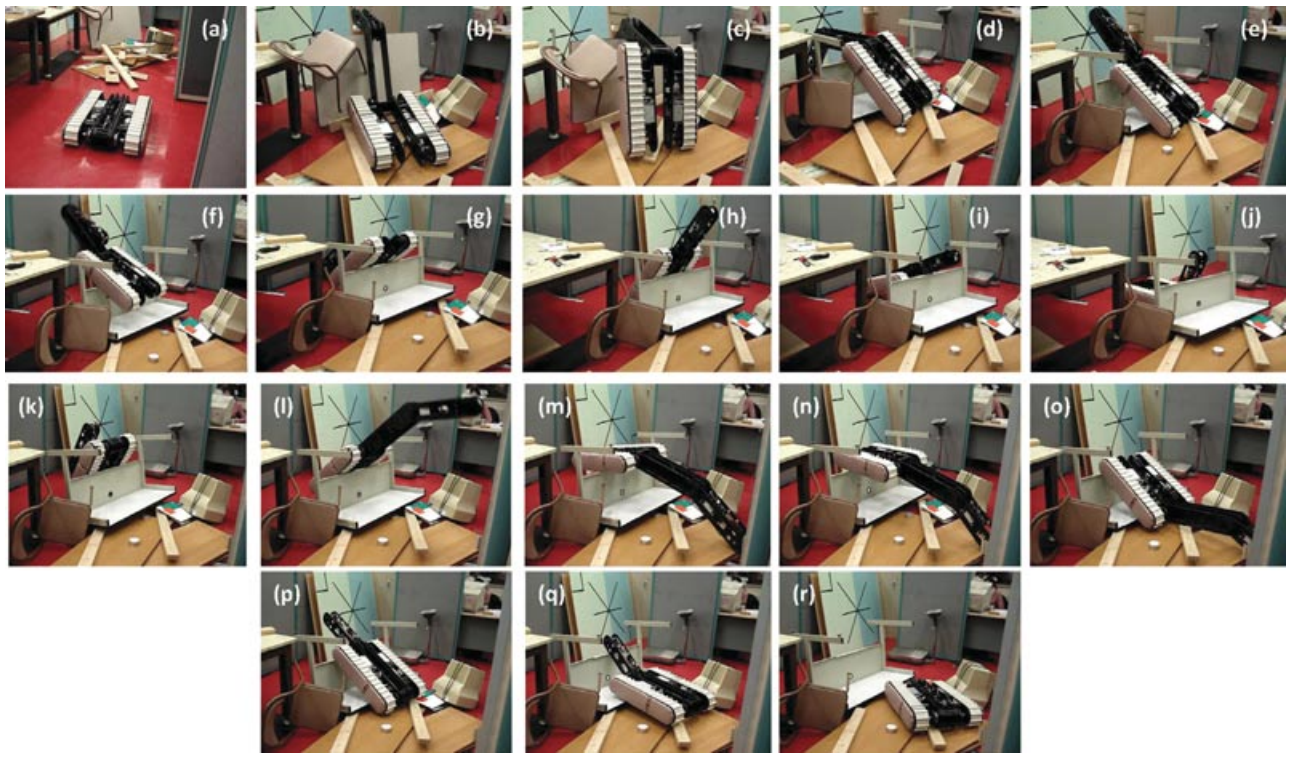

Figure 22. Combined mobility configurations for rubble pile traversal.

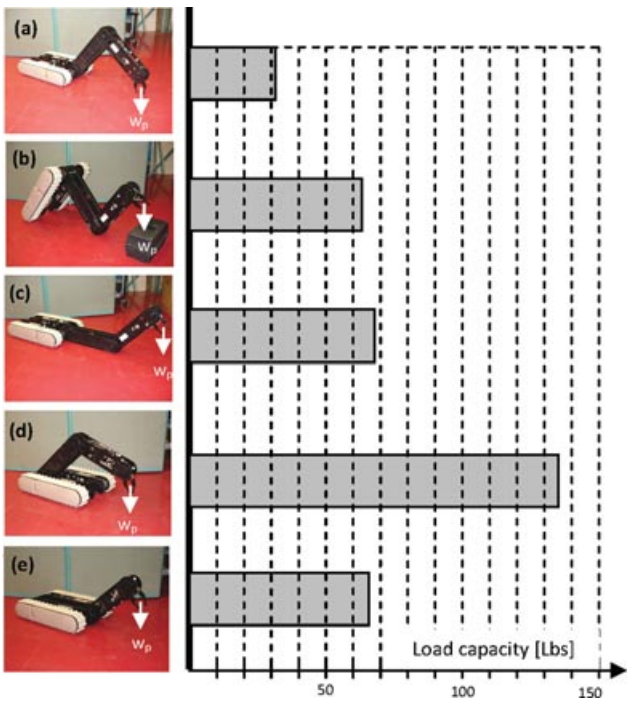

Figure 23. Configurations for manipulation.

(i) The robot tries to lift a load with the gripper (a).
(ii) The base link tracks rotate 180 deg to provide the countertorque until they touch the ground [(b)–(e)].
(iii) The robot lifts the object with its new configuration (f).

It is interesting to observe that the robot's motion steps from configuration (a) to configuration (f) shown in Figure 24 are equivalent to the robot automatically changing its configuration from its "weakest" (easily loses balance) as shown in Figure 23(a) to its "strongest" (structurally more robust to tip-over instability) as shown in Figure 23(d). Consequently, according to the graph shown in Figure 23, the robot is automatically increasing its end-effector capacity from 14 kg (~31 lb) to 61 kg (~135 lb).

The adaptable manipulation capability is a direct outcome of the new design, namely (i) the hybrid nature of the platform and manipulator arm and their ability to be interchangeable in their roles; and (ii) the articulated structure of the robot mechanism and its ability to relocate its COG to provide or compensate for the required counterforce moment. This type of "adaptable manipulation" can be done with other manipulation configurations shown in Figure 23. For instance, the robot mechanism can change its configuration (while holding an object at the end effector) from (e) to (c) as shown in Figure 23, by rotating the base

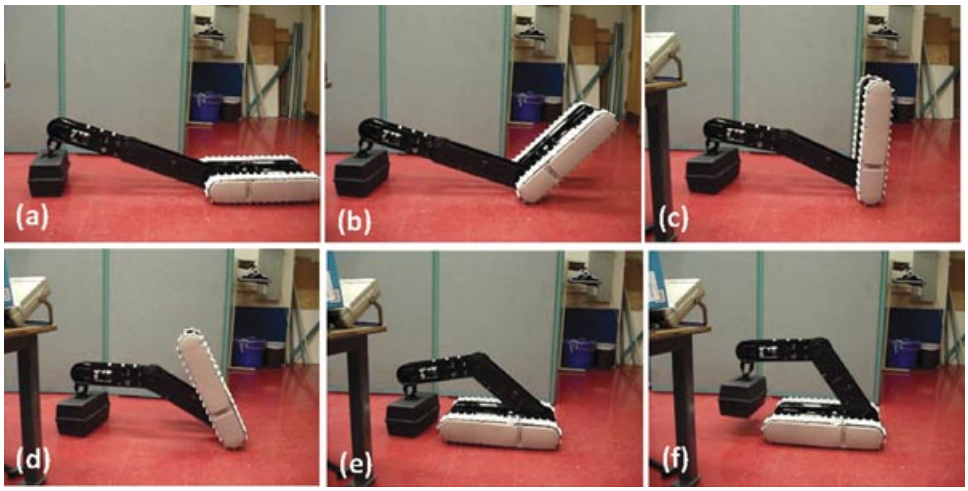

Figure 24. Adaptable manipulation configuration steps.

link tracks 180 deg to the back in order to provide greater reach to the manipulated object.

6. CONCLUSIONS

This paper focused on presenting extensive experimental results and testing of a new mobile robot design in order to assess its overall mobility and manipulation characteristics. The new mobile robot design was based on hybridization of the mobile platform and manipulator arm mechanisms as one entity for robot locomotion as well as manipulation. The tests were performed on an obstacle course that consisted of various test rigs including man-made and some natural obstructions as a representative subset of the possible hindrances to robot cross-country movement. The entire range of the HMR's locomotion and manipulation modes was successfully experimented and validated.

Figures 4 and 5 show how the different links constituting the HMR system can be used for both locomotion and manipulation purposes in several modes of operation (as discussed in Section 3). These functions of locomotion, manipulation, and hybrid locomotion and manipulation have been utilized to demonstrate a large variety of unique and very challenging practical tasks the mobile robot was able to perform. These new functionalities could be potentially used in a vast variety of pertinent applications, such as search and rescue missions, reconnaissance, inspection, surveillance, planetary exploration, and police and military tasks, mainly owing to the robot's ability to provide new locomotion and manipulation capabilities that greatly help to overcome challenging obstacles that would be typically encountered in such applications.

Some of the tasks presented herewith are summarized as follows: traversing tall cylindrical obstacles (up to 0.6 m); climbing and descending stairs (variety of slopes, materials, and sizes); climbing and descending tall obstacles (up to 0.75 m); crossing ditches (up to 0.7 m); lifting (up to 61 kg or 135 lb) and carrying (at least 187 kg or 410 lb) tasks; and tasks that require simultaneous manipulation and climbing/descending of obstacles. The HMR's versatile and agile functionalities have also shown an ability to traverse rubble piles, which also demonstrate the durability characteristics of the new design. The robot's articulated structure has also demonstrated a unique ability to provide "adaptable" manipulation autonomously, namely to automatically change its link configuration (COG location) and thereby increase its resistance for tip-over instability as shown in Figure 24.

As a future work, some of the limitations pertaining to the design of the robot could be improved, such as redesigning the data RF flat antennas to allow omnidirectional power radiation and thereby greatly increase the wireless data communication range and redesigning the gripper mechanism by adding a roll DOF in order to be able to open doors with circular knobs. Furthermore, we are currently developing a new prototype with new control hardware and sensing capabilities in order to enable semiautonomous functions to the mobile robot and perform more field tests that also incorporate semiautonomous functionalities.

ACKNOWLEDGMENT

This work was partially supported by the Natural Sciences and Engineering Research Council of Canada (NSERC) and Engineering Services, Inc., of Toronto, Canada.

REFERENCES

Angeles, J. (2005). An innovative drive for wheeled mobile robots. IEEE/ASME Transactions on Mechatronics, 10(1), 43–49.

Ben-Tzvi, P. (2008). Hybrid mobile robot system: Interchanging locomotion and manipulation. Ph.D. dissertation, Department of Mechanical and Industrial Engineering, University of Toronto, Toronto, Ontario, Canada.

Ben-Tzvi, P., Goldenberg, A.A., & Zu, J.W. (2007a, August). A novel control architecture and design of hybrid locomotion and manipulation tracked mobile robot. In Proceedings of the 2007 IEEE International Conference on Mechatronics and Automation (ICMA 2007), Harbin, China (pp. 1374–1381).

Ben-Tzvi, P., Goldenberg, A.A., & Zu, J.W. (2007b, October). Implementation of sensors and control paradigm for a hybrid mobile robot manipulator for search and rescue operations. In Proceedings of the 2007 IEEE International Workshop on Robotic and Sensors Environments (ROSE 2007), Ottawa, Ontario, Canada (pp. 92–97).

Ben-Tzvi, P., Goldenberg, A.A., & Zu, J.W. (2008a, May). Design, simulations and optimization of a tracked mobile robot manipulator with hybrid locomotion and manipulation capabilities. In Proceedings of the 2008 IEEE International Conference on Robotics and Automation (ICRA'08), Pasadena, CA.

Ben-Tzvi, P., Goldenberg, A.A, & Zu, J.W. (2008b). Design and analysis of a hybrid mobile robot mechanism with compounded locomotion and manipulation capability. Journal of Mechanical Design, 130(7), 1–13.

Ben-Tzvi, P., Raoufi, C., Goldenberg, A.A., & Zu, J.W. (2007, October). Virtual prototype development and simulations of a tracked hybrid mobile robot. In Proceedings of MSC. Software 2007 Virtual Product Development Conference, Detroit, MI.

Costo, S., & Molfino, R. (2004, March). A new robotic unit for onboard airplanes bomb disposal. In 35th International Symposium on Robotics ISR 2004, Paris (pp. 23–26).

Foster-Miller (2010). TALON mobile robot. Retrieved February 16, 2010, from http://www.foster-miller.com/lemming.htm.

Goldenberg, A.A., & Lin, J. (2005). Variable configuration articulated tracked vehicle. US Patent #7600592.

Guarnieri, M., Debenest, P., Inoh, T., Fukushima, E., & Hirose, S. (2005). Helios VII: A new vehicle for disaster response, mechanical design and basic experiments. Advanced Robotics, 19(8), 901–927.

Hirose, S., Fukushima, E.F., Damoto, R., & Nakamoto, H. (2001, November). Design of terrain adaptive versatile crawler vehicle HELIOS-VI. In Proceedings IEEE/RSJ International Conference on Intelligent Robots and Systems, Maui, HI (pp. 1540–1545).

Iwamoto, T., & Yamamoto, H. (1990). Mechanical design of variable configuration tracked vehicle. Transactions of the ASME—Journal of Mechanical Design, 112, 289–294.

Kennedy, B., Agazarian, H., Cheng, Y., Garrett, H.G., Huntsberger, T., Magnone, L., Mahoney, C., Meyer, A., & Knight, J. (2001). LEMUR: Legged Excursion Mechanical Utility Rover. Autonomous Robots, 11(11), 201–205.

Michaud, F., Létourneau, D., Paré, J.-F., Legault, M.-A., Cadrin, R., Arsenault, M., Bergeron, Y., Tremblay, M.-C., Gagnon, F., Millette, M., Lepage, P., Morin, Y., & Caron, S. (2003, September). Co-design of AZIMUT, a multi-modal robotic platform. In ASME 2003 Design Engineering Technology Conferences and Computers and Information in Engineering Conference, Chicago, IL.

Munkeby, S., Jones, D., Bugg, G., & Smith, K. (2002, April). Applications for the MATILDA robotic platform. In Proceedings of SPIE—Unmanned Ground Vehicle Technology IV, Orlando, FL (vol. 4715, pp. 206–213).

Purvis, J.W., & Klarer, P.R. (1992, August). RATLER: Robotic All Terrain Lunar Exploration Rover. In Proceedings Sixth Annual Space Operations, Applications and Research Symposium, Johnson Space Center, Houston, TX (pp. 174–179).

Saranli, U., Buehler, M., & Koditschek, D.E. (2001). RHex: A simple and highly mobile hexapod robot. International Journal of Robotics Research, 20(7), 616–631.

Wang, D., & Low, C.B. (2008). Modelling and analysis of skidding and slipping in wheeled mobile robots: Control design perspective. IEEE Transactions on Robotics, 24(3), 676–687.

White, J.R., Sunagawa, T., & Nakajima, T. (1989, September). Hazardous-duty robots—Experiences and needs. In Proceedings IEEE/RSJ International Workshop on Intelligent Robots and Systems '89 (IROS '89), Tsukuba, Japan (pp. 262–267).

Yamauchi, B. (2004, April). PackBot: A versatile platform for military robotics. In Proceedings of SPIE—Unmanned Ground Vehicle Technology VI, Orlando, FL (vol. 5422, pp. 228–237).